S-II STAGE VIBRATION TESTING AND ANALYSIS FOR THE POGO PHENOMENA

By

H. M. Lee

SUMMARY

The Dynamics Analysis Branch of the Astronautics Laboratory of Marshall Space Flight Center conducted an investigation of the longitudinal oscillation problem encountered during second stage burn of the Saturn V vehicle. This report describes the structural test and math modeling effort that was undertaken. It includes details of the extensive experimental research program performed on the S-II stage vehicle in conjunction with a definitive math model development utilizing the test information.

The tests were conducted using a shortened S-II stage to determine dynamic characteristics of the thrust structure/center engine crossbeam/liquid hydroelastic system. These data were used as direct input in developing the math model. Comparisons between results obtained from the empirical model and tests are made; these show excellent correlation in frequency, response, and mass characteristics. Also, comparisons between flight data and the calculated overall vehicle modal parameters are made to further verify the adequacy of the structural model.

INTRODUCTION

Development of large space vehicles involves the assemblage of vast amounts of hardware. Structural convergence of these components, in most cases, produces an operational system with many dynamically complex characteristics. The inflight dynamic response of these vehicles is dependent on parameters related to structural design, fluid mechanics, propulsion mechanisms, and control systems. To properly analyze dynamic problems that occur during flight, all of these effects must be taken into account.

On December 21, 1968, the first manned Saturn V vehicle (AS-503) was launched. Second stage longitudinal oscillation problems, known as POGO were first recorded during this flight. The severity of this problem did not become apparent, however, until the flight of AS-504 (Apollo 9 mission) on March 3, 1970. Figure 1 shows recorded accelerometer response in G's versus flight time for three areas in the aft end of the S-II stage. These data were taken from oscillograms of the AS-504 lox sump, center engine, and outboard engine during S-II stage burn.

An analysis of this flight data and some previous test data revealed that the center engine crossbeam responded at a frequency near 18 Hz throughout flight. The response of the beam was of low amplitude until near the end of second stage burn. At this time the system became unstable, and the large amplitude oscillations shown in Figure 1 were encountered. It was hypothesized that one of the predominant lox bulkhead modes increased in frequency with decreasing liquid level and coupled with the crossbeam resonance to cause this instability. This would apparently indicate that as the lox bulkhead frequency approached the 18 Hz region, the total system would enter into a closed loop, regenerative mode, producing high response levels in the aft section of the S-II stage.

Because of the impact and complexity of the problem, an extensive experimental program was initiated. Figure 2 exhibits a flow chart outline of the total S-II oscillation program. This paper presents, however, only a summary of the testing, modeling techniques, and data comparisons utilized in updating, assessing, and verifying the structural model.

DESCRIPTION OF TESTS

Dynamic testing of the S-II stage was composed of three phases. Figure 3 shows the structural differences between the three phases as well as the method of dynamic excitation. The approximate location of the accelerometer instrumentation is also shown for each case. It should be noted that for phase I testing, the aft skirt was fixed to ground, but during phase II and III testing the structure was

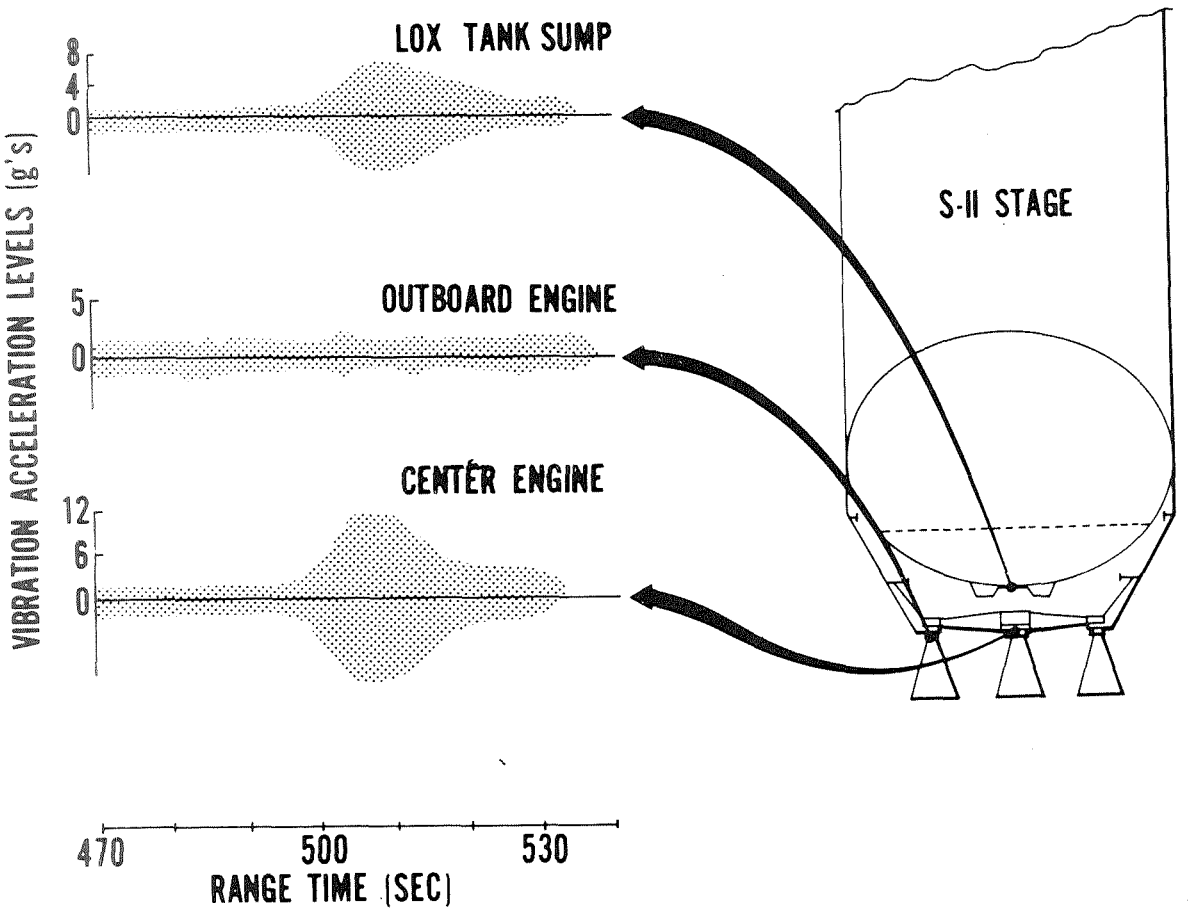

Figure 1. AS-504 vibration amplitudes.

supported on a low frequency air suspension system. The lox tank was filled with de-ionized water and drained in several incremental levels. Modal surveys, which include sinusoidal sweeps from 5 to 50 Hz and resonant frequency dwell tests, were then performed at each of the levels.

The primary objective of the phase I sequence was to empirically investigate the axisymmetric modes of the aft lox tank bulkhead as a function of propellant level, corresponding to levels prior to and through the period of longitudinal oscillation observed during the AS-504 flight. The investigation included the acquisition of such dynamic parameters as mode shapes, damping frequency, generalized mass, and tank bottom pressures. The phase II and phase III test efforts were designed to determine bulkhead/thrust structure/crossbeam modal interaction. Phase III also included the installation of the five lox feedlines capped and filled with water. The goal of these two phases was to determine the following properties: (1) predominant system mode shapes, (2) system damping, (3) modal frequencies, (4) generalized mass, (5) effects of the lox feedlines, and (6) tank bottom/lox line pressures.

The phase I test proved to be an excellent setup for determining the axisymmetric hydroelastic modes of the lox tank bulkhead. Accelerometers were placed along several meridians over a 180-degree section of the bulkhead. Response data obtained at the same level on each meridian were then averaged to yield mode shapes. Figure 4 shows the first three bulkhead resonant frequencies versus flight time as related to the AS-504 vehicle S-II stage burn.

Phase II and III data were obtained from the structural interaction of the lox tank bulkhead, aft

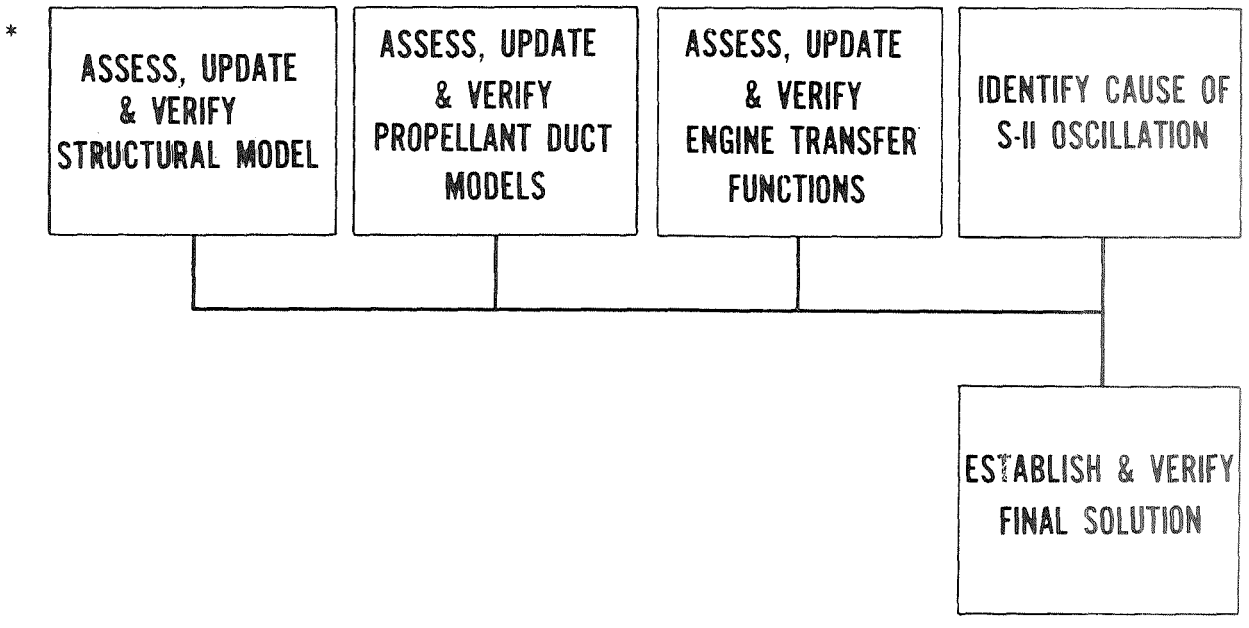

Figure 2. S-II oscillation overall program flow.

skirt, thrust structure, center engine crossbeam, and several other components. Presented in Figure 5 are the first five longitudinal S-II system modal frequencies versus AS-504 second stage flight time. Interesting modal frequency patterns can be noted in the figure because of the complex interaction of the structural components. These frequency versus time plots represent only one of the many types of forced response information obtained from the S-II testing program. It was from the data that the math model of the aft end of the S-II vehicle was defined.

MATH MODELING TECHNIQUE

A multi-degree-of-freedom model of the phase I test configuration was developed to simulate the response of the structure/fluid system. The modeling technique used is given in Reference 1. The structure and fluid were assumed to be a damped structural system subjected to harmonic forced motion. Test response data are used as direct input to the equation of motion, from which the uncoupled mode shapes are obtained. The corresponding mass and stiffness matrices can be calculated using the condition of orthogonality of modes.

The phase II modeling utilized the same technique as described above, incorporating not only the lox tank but also the thrust structure, outboard engine, and center engine crossbeam. The governing differential equation in generalized coordinates is

$$\{\ddot{q}_n\} + [2\zeta_n \omega_n]\{\dot{q}_n\} + [\omega_n^2]\{q_n\} = \left[\frac{1}{Mg_n}\right][\phi]^T \{F \sin \omega t\} \quad , \tag{1}$$

where

q_n = nth model coordinate

ω_n = natural frequency of nth mode

$\{\phi\}_n$ = nth modal column

$\{F \sin \omega t\}$ = applied force at frequency ω

ζ_n = damping of nth mode

Mg_n = generalized mass of nth mode.

The steady-state solution of equation (1) is

$$q_n = \frac{\left(\frac{\phi_{rn} F_{rn}}{Mg_n \omega_n^2}\right) \sin(\omega t + \psi_n)}{\left\{\left(1 - \frac{\omega^2}{\omega_n^2}\right)^2 + \left(2\zeta_n \frac{\omega}{\omega_n}\right)^2\right\}^{1/2}} \tag{2}$$

PHASE I - EXCITATION THRU LOX TANK SUMP

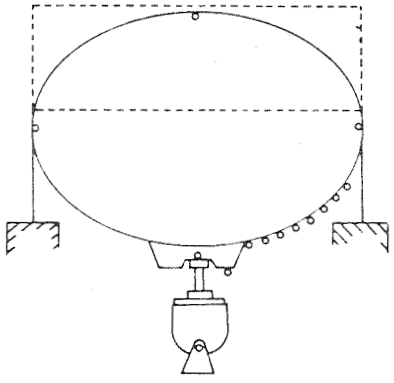

PHASE II - EXCITATION THRU CENTER ENGINE WITHOUT FEEDLINES

PHASE III - EXCITATION THRU CENTER ENGINE WITH FEEDLINES

° ACCELEROMETER

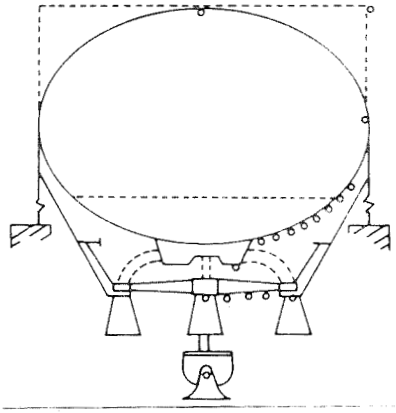

DYNAMIC PARAMETERS OBTAINED - FREQUENCY GENERALIZED MASS PRESSURES DAMPING MODE SHAPES

Figure 3. Test definition.

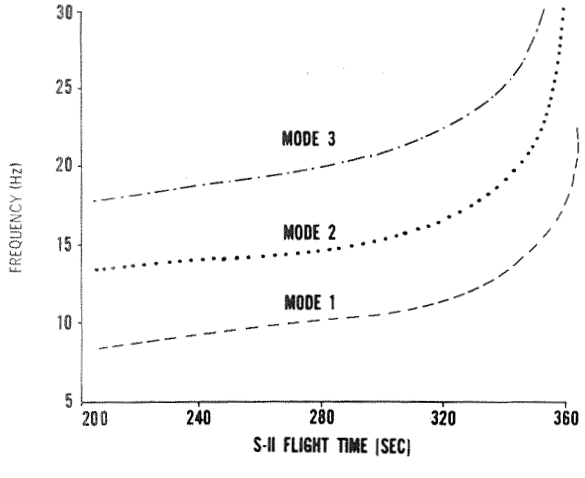

Figure 4. Phase I frequency versus time.

in which

$$\psi_n = \tan^{-1}\left[\frac{2\zeta_n \frac{\omega}{\omega_n}}{1 - \frac{\omega^2}{\omega_n^2}}\right]$$

and

$$q_n = \frac{X_{Sn}}{\phi_{Sn}}$$

where

F_{rn} = applied force at point r in the nth mode

ϕ_{rn} = modal displacement at point r in the nth mode

ϕ_{Sn} = modal displacement at point S in the nth mode

X_{Sn} = real displacement at point S in the nth mode.

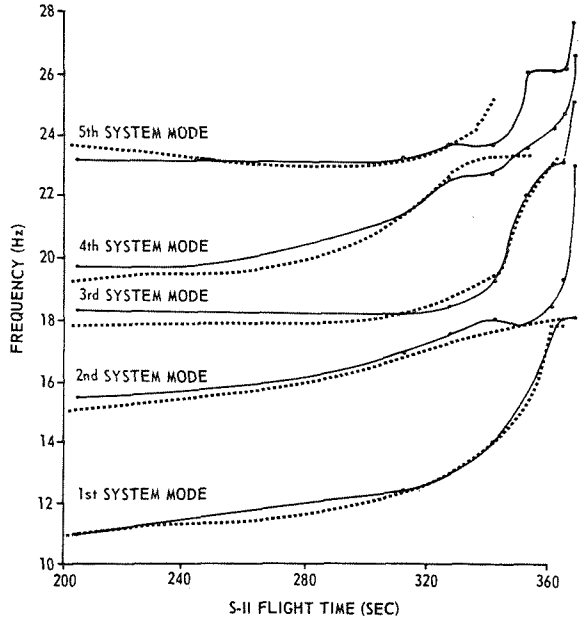

Figure 5. Phase II and III frequency versus time.

This substitution then results in the following equation:

$$\frac{X_{Sn}}{F_{rn}} = \frac{\left(\frac{\phi_{rn}\,\phi_{Sn}}{Mg_n\,\omega_n^2}\right)\sin\,(\omega t + \psi_n)}{\left\{\left(1 - \frac{\omega^2}{\omega_n^2}\right)^2 + \left(2\zeta_n\frac{\omega}{\omega_n}\right)^2\right\}^{1/2}} \qquad (3)$$

If $\frac{X_{Sn}}{F_{rn}}$ is treated as forced response, one can assume that it is comprised of the summation of the response contributions from each mode being analyzed. With this in mind, the following system of equations is obtained for response with an applied force at mode 1 with a forcing frequency of $\omega = \omega_1$:

$$C_{11}\phi_{11}^2 + C_{12}\phi_{12}^2 + \ldots + C_{1n}\phi_{1n}^2 = \frac{X_1}{F_1}$$

$$C_{11}\phi_{11}\phi_{21} + C_{12}\phi_{12}\phi_{22} + \ldots + C_{1n}\phi_{1n}\phi_{2n} = \frac{X_2}{F_2}$$

$$\vdots \qquad\qquad \vdots$$

$$C_{11}\phi_{11}\phi_{n1} + C_{12}\phi_{12}\phi_{n2} + \ldots + C_{1n}\phi_{1n}\phi_{nn} = \frac{X_n}{F_1}$$

The constants C_{ij} represent the coefficients of the modal displacement products $\phi_{rn}\,\phi_{sn}$ seen in equation (3). The subscripts i and j refer to the forcing frequency ω_i and the modal resonant frequency ω_j, respectively. C_{ij} can be more specifically defined as follows:

$$C_{ij} = \frac{1}{\omega_j^2}\,\frac{\sin\,(\omega_i t + \psi_j)}{\left\{\left(1 - \frac{\omega_i^2}{\omega_j^2}\right)^2 + \left(2\zeta_j\frac{\omega_i}{\omega_j}\right)^2\right\}^{1/2}} \qquad (4)$$

A similar set of equations may be obtained for every forcing frequency $\omega = \omega_i$ to $\omega = \omega_n$.

Careful examination of equation (4) reveals that the modal displacements are the only unknowns. All other parameters can be obtained for the test data. These unknowns $\left[\phi_{rm}\;\phi_{Sn}\right]$ supply the information needed to define independent normal modes $[\phi]$ for the system.

Utilizing the conditions of orthogonality, the mass and stiffness matrices can be found in the following manner:

$$[M] = \left[\phi^T\right]_n^{-1}\left[Mg_n\right]\left[\phi\right]_n^{-1} \qquad (5)$$

$$[K] = \left[\phi^T\right]_n^{-1}\left[Mg_n\omega_n^2\right]\left[\phi\right]_n^{-1} \qquad (6)$$

Several fill conditions were selected from each test phase. Modal frequencies, normal displacements, damping, and generalized mass from the dwell test data were input into equation (1), and normal modes were then substituted into equations (5) and (6).

COMPARISON OF TEST AND MODEL DATA

One check made on the developed model was a comparison of calculated response versus frequency with frequency response data obtained from the test. The model was derived using data obtained at resonant dwell points. As expected, exact agreement was shown at those points, as seen in Figures 6 and 7 for phase I and phase II comparisons, respectively. Also good agreement is shown at points other than resonance through the entire frequency range of interest. This indicates that the model adequately simulated the hydroelastic test system.

The total longitudinal mass of the system was determined from the generated mass matrices and is shown in Table 1 for the Phase II conditions. The total mass check was important, since this model

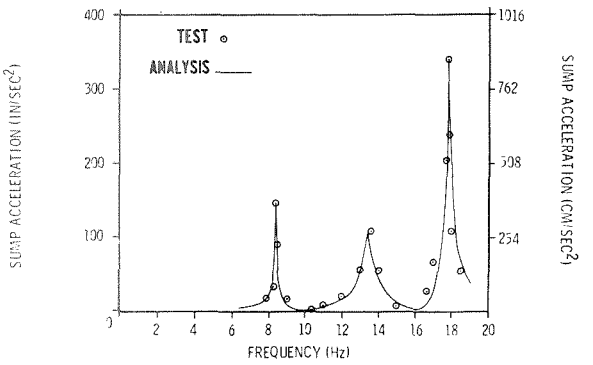

Figure 6. Phase I — model/test comparison (205-sec flight time).

would eventually be incorporated into a flight model of the Saturn V vehicle. No restraint had been placed on the magnitude of the mass matrix, but the table shows good agreement with actual test vehicle weights.

COMPARISON OF VEHICLE ANALYSIS AND FLIGHT DATA

It should be noted that the phase III test data were not used in deriving a final model for use in vehicle analysis. A comparison between the phase II and phase III data did not reveal an anomaly induced by the addition of engine feedlines. It was, therefore, concluded that the line definition that had been previously used would be incorporated and that phase II data adequately defined the thrust structure/

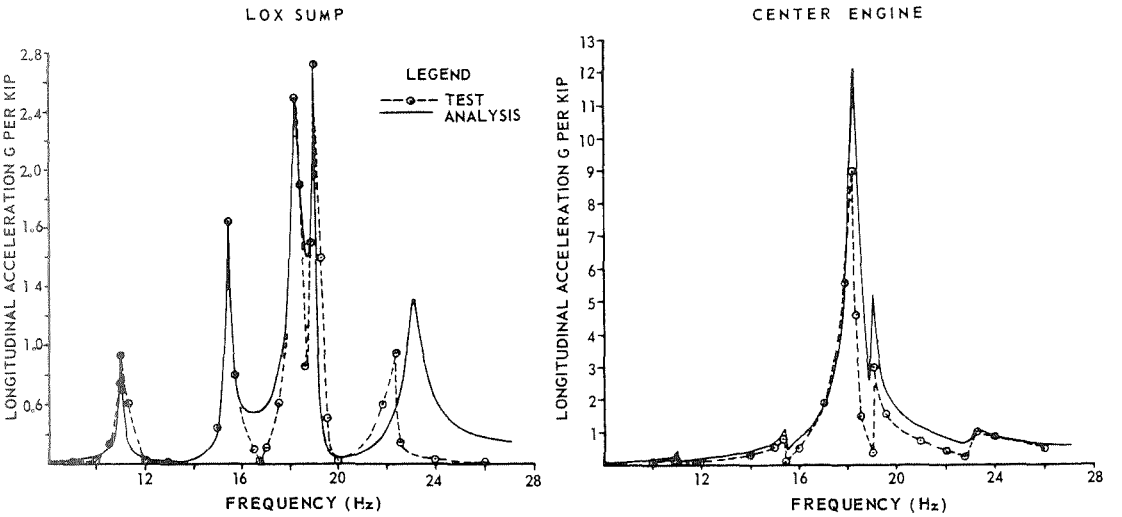

Figure 7. Phase II — model/test comparison (205-sec flight time).

TABLE 1. COMPARISON OF ACTUAL WEIGHTS WITH WEIGHTS CALCULATED FROM MASS MATRICES

S-II Flight Time, sec	Actual Weight, kg (lb)	Mass Matrix Weight, kg (lb)	Percent Error
205	207 445 (457 330)	218 051 (480 711)	+5.11
313	97 447 (214 830)	119 750 (264 000)	+22.8
328	84 001 (185 187)	82 826 (182 597)	-1.39
341	72 489 (159 588)	71 851 (155 977)	-2.26
352	62 882 (138 629)	62 847 (138 332)	-0.02
361	55 772 (122 954)	55 903 (123 243)	+0.02
364	52 853 (116 496)	52 759 (116 311)	-0.01
370	50 197 (110 663)	51 482 (113 496)	+2.56

center engine crossbeam/bulkhead system. A model derived from these data was then incorporated into the total Saturn V vehicle (Fig. 8), which contains spring-mass representations of the remaining flight structure. Figure 9 shows a comparison of a frequency analysis of the Saturn V S-II stage burn model versus AS-504, AS-507, and AS-508 flight data. The first three modes seen on the chart are major vehicle longitudinal modes. The next three modes represent the first and second predominant bulkhead modes and the predominant crossbeam mode, respectively. It is apparent that the flight data generally follow the predominant second bulkhead mode. However, no definite conclusion can be drawn from this analysis, since such parameters as forcing function, control systems, and engine transfer functions were not incorporated.

Approximate flight time for the POGO instability on AS-504 was at 340 seconds into the S-II stage burn. The AS-507 flight did not experience this instability because of the center engine shutdown at about 60 seconds, before the end of S-II burn. This was done to open the unstable regenerative loop developed on flights such as AS-504. The AS-508 flight also had a scheduled early center engine shutdown; however, POGO developed at about 170 seconds into S-II burn, and an unscheduled center engine shutdown was effected because of excessive vibration levels.

CONCLUSIONS

It has been shown that the aft end of the S-II stage, including such complex components as bulkhead/fluid, thrust structure engines, and cross-beam, was successfully tested and mathematically

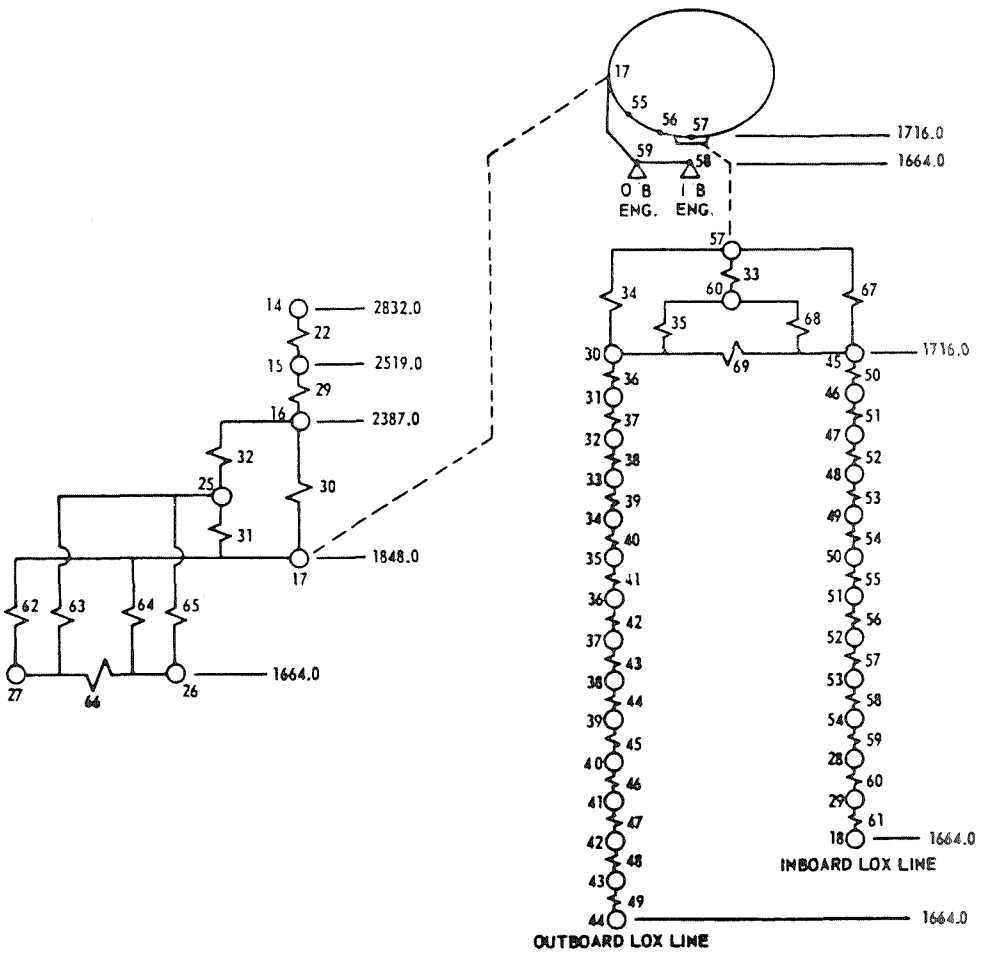

Figure 8. S-II flight model.

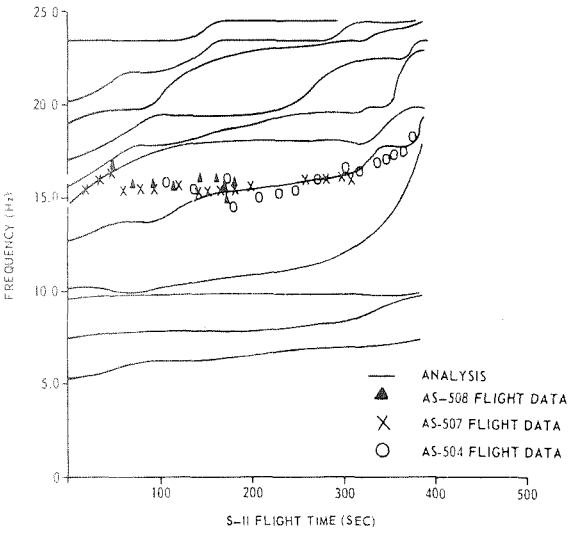

Figure 9. Flight data versus flight model.

modeled. The results yielded an excellent frequency response and mass characteristics correlation. These models were incorporated into overall flight vehicle models and analyzed for modal parameters. Preliminary comparisons of frequency analysis with actual flight data indicate that the total structural modeling program has produced a good representation of the flight vehicle. Actual POGO instability analyses will be performed later utilizing these test-developed models along with other propulsion and control system transfer function modeling data. Future Saturn V flight vehicles will also be evaluated for this oscillatory problem when the model is able to reproduce all responses observed on previous vehicles.

REFERENCE

1. Thoren, A. R.: Preliminary Evaluation of S-II Mini-Test Results. Brown Engineering Technical Letter ASD-ASTNL-706, Huntsville, Alabama, 1969.